ISSN 1061-933X, Colloid Journal, 2022, Vol. 84, No. 6, pp. 663–671. © Pleiades Publishing, Ltd., 2022.
Russian Text © The Author(s), 2022, published in Kolloidnyi Zhurnal, 2022, Vol. 84, No. 6, pp. 695–704.

The Use of Size-Exclusion Chromatography and Laser Desorption/Ionization for Studying Silver Nanoparticles Synthesized in Reverse Micelles

S. A. Borovikova[a], *, A. D. Shafigulina[a], A. A. Revina[a], and A. K. Buryak[a]

[a] *Frumkin Institute of Physical Chemistry and Electrochemistry, Russian Academy of Sciences, Moscow, 119071 Russia*

**e-mail: borovikova7@mail.ru*

Received June 16, 2022; revised August 11, 2022; accepted August 11, 2022

Abstract—Mass spectrometry with matrix/surface-assisted laser desorption/ionization has been employed to confirm the formation of nanoparticles as a result of the synthesis in water/AOT/isooctane reverse micellar solutions. Mass spectra have been obtained for Ag_n, as well as $Ag_n \cdot Na^+$ and $Ag_n \cdot Na \cdot H^+$ adducts, where n = 1–20. Size-exclusion chromatography has been used to perform a year-long study of the size characteristics of silver nanoparticles. It has been found that silver nanoparticles synthesized in reverse micellar solutions are mainly represented by two fractions. The particles of one fraction have sizes of 1–6 nm, which can remain almost unchanged when being stored for a long time. The formation of the coarse fraction with particle sizes of 15–32 nm is a reversible process, during which particle sizes vary within a range of ±10 nm. The obtained data have led to an assumption that reverse micellar solutions with degrees of hydration up to 20 are stable systems, other synthesis conditions being equal, while the particles of the coarse fraction are aggregates of the fine-fraction particles, which retain their stabilizing shells of AOT molecules upon aggregation.

DOI: 10.1134/S1061933X22700119

INTRODUCTION

At present, nanoparticles (NPs) of different natures provoke scientific and practical interest due to their unique properties. The main reason for a change in the physical and chemical properties of nanoparticles is an increase in the fraction of "surface" atoms, while, from the energetic point of view, a decrease in the particle size leads to an increase in the role of surface energy [1, 2].

Silver NPs are of substantial interest, because they are widely used for the preparation of antimicrobial and catalytically active composites [3, 4], electrochemical sensors [5], and polyethylene nanofibers [6]. Owing to their antimicrobial properties, silver NPs are applied for producing medical equipment and tools [7]. Moreover, they are intensively studied with the aim of their use in metallurgy for the production of Ag-containing stainless steel with a unique microstructure [8].

One of important problems encountered when synthesizing NPs in solutions is the prevention of their coagulation. NPs are stabilized by adding various surfactants and their mixtures, soluble polymers, and other stabilizers to the media used for their synthesis. Variations in the synthesis conditions enable one to regulate the sizes and, in some cases, the shapes of obtained NPs [9, 10].

One of the most popular methods used to obtain stable NPs of different compositions is their synthesis in reverse micelles, which are nanosized water droplets stabilized with surfactant molecules in a liquid hydrophobic phase [11, 12]. This method of the synthesis yields NPs that are time-stable and have a narrow size distribution, with these properties predetermining and widening the fields of their practical application [13, 14]. Therefore, the question as to the duration of the stability of diverse nanoparticles synthesized in reverse micelles is very urgent.

The methods of liquid chromatography and mass spectrometry give broad possibilities of studying the chemical composition and size characteristics of NPs formed in micelles, because these methods enable one to study nanoparticles in reverse micellar solutions (RMSs) with no laborious sample preparation. This markedly reduces analysis duration and excludes possible changes in the structure and properties of the obtained NPs [15]. Mass spectrometry is a method that makes it possible to detect the existence of nanoparticles, water pools, and stabilizing shells formed by surfactant molecules. When using this method, mild ionization methods are employed to maximally overcome the main problem concerning the fragmentation of NPs and the loss of protective ligands upon ionization [16–19].

Size-exclusion chromatography (SEC) enables one to determine the sizes of synthesized NPs and perform their preparative fractionation over sizes [13]. Moreover, the average particle diameters measured by the SEC method are in good agreement with the data of atomic force and transmission electron microscopy, thereby making this method promising and reliable for determining the sizes of NPs of various metals and their variations with time [13, 20]. The goal of this work is to study silver nanoparticle sizes and their time variations by the mass spectrometry and size-exclusion chromatography methods to optimize their synthesis and control their stability in the course of storage.

EXPERIMENTAL

As objects for the study, we selected six samples of silver NPs, which had been obtained by radiochemical synthesis in reverse micelles [21–23]. As initial reagents, we used an aqueous 0.3 M solution of $Ag[NH_3]_2NO_3$ complex salt and a 0.15 M solution of a surfactant, sodium bis(2-ethylhexyl) sulfosuccinate (AOT) (Sigma-Aldrich USP, 99%), in isooctane with hydration degrees ω corresponding to ratios $[H_2O]/[AOT] = 2, 4, 8, 16$, and 20. The prepared solutions were stored at room temperature in the dark for a year.

The formation of NPs in reverse micellar solutions was confirmed using the analysis performed by the method of laser desorption/ionization (LDI). A reverse micellar solution of a silver salt, $Ag[NH_3]_2NO_3$, which is a precursor for NP synthesis, and Ag NPs in an RMS were applied onto an inert substrate in the initial form and dried in air. Previously [15, 24], it was shown that the drying followed by dissolution of nanoparticles does not change their composition and structure. The study was carried out using a Bruker Daltonics Ultraflex II mass spectrometer equipped with a nitrogen laser operating at a wavelength of 337 nm. Pulse frequency was varied within a range of 5–20 Hz, the number of pulses was 25–100, and the laser pulse energy was 110 μJ. Ions were detected in the reflectron mode with the registration of positive and negative ions.

Nanoparticle sizes, as well as their variations and stability in time, were determined by SEC for a year [13]. The frequency of the measurements was decreased with an increase in the duration of RMS storage, because it was assumed that the solutions were equilibrated with time.

The SEC experiments were performed using a liquid chromatograph equipped with a Knauer WellChrom K-12 pump. Tetrahydrofuran (Panreac) was used as a mobile phase; its flow rate through a Waters UltraStyragel 10^3 Å column (pore size of 100 nm) was 0.65 cm^3/min. The detection was performed with a Kratos spectrophotometric detector operating at λ = 420 nm.

The NP sizes were recalculated by the following empirical equation [25] through the sizes of polystyrene references (PSRs), which were used for calibration:

$$d\,(\text{Å}) = 0.274 M_w^{0.589},$$

where M_w is the weight-average mass of PSR (Da) determined from a calibration plot and d is the diameter (Å) of a conventionally spherical particle of PSR with a corresponding molecular mass.

RESULTS AND DISCUSSION

Figures 1 and 2 show the mass spectra recorded for Ag NPs in an RMS (ω = 8) within an m/z range of 60–3600. Ag_n adducts of silver and Ag_nNa^+ and Ag_nNaH^+ adducts, where $n = 1$–21, were found, and mass m/z = 553 (peak 12) was recorded that corresponded to an AOT molecule cationated with an Ag^+ ion.

For comparison, Fig. 3 presents the mass spectrum of a silver salt, $Ag[NH_3]_2NO_3$, which was used as an initial reagent for the synthesis of NPs.

Peaks 1, 5, and 6 in the mass spectrum correspond to silver clusters with the numbers of atoms up to three; peaks 3 and 4 are attributed to Na_2SO_3 molecules cationated with Na^+ and K^+ ions, respectively; and peak 10 is assigned to a molecule of the surfactant (AOT) cationated with Na^+ ions. It should be noted that the formation of larger silver clusters with numbers of atoms larger than three was not recorded in this mass spectrum.

The composition of the products found in the mass spectra of the silver salt and the RMS of Ag NPs (ω = 8) is described in detail in Table 1.

It follows from Figs. 1 and 2 and Table 1 that the ionization of the components of the sample of Ag NPs in the RMS yields a wide spectrum of silver cluster ions and adducts with AOT components. For example, peak 19 with m/z 1356 corresponds to a trimer of AOT molecules cationated with a Na^+ ion. The appearance of silver clusters with a number of atoms as large as 21 is, most probably, an intermediate state of the formation of nanosized Ag particles in the course of their synthesis. In [26, 27], silver nanoclusters were identified by mass spectroscopy as nuclei of nanoparticles during their synthesis and the mechanisms of their formation were determined. The data obtained have led to the conclusion that mass spectrometry may be used to study the processes of clustering that accompany the ionization of Ag NPs synthesized in RMSs.

The works devoted to studying the physicochemical properties of silver nanoparticles [9, 13] in RMSs have shown that they exhibit absorption bands predominantly in the UV (~250 nm) and visible

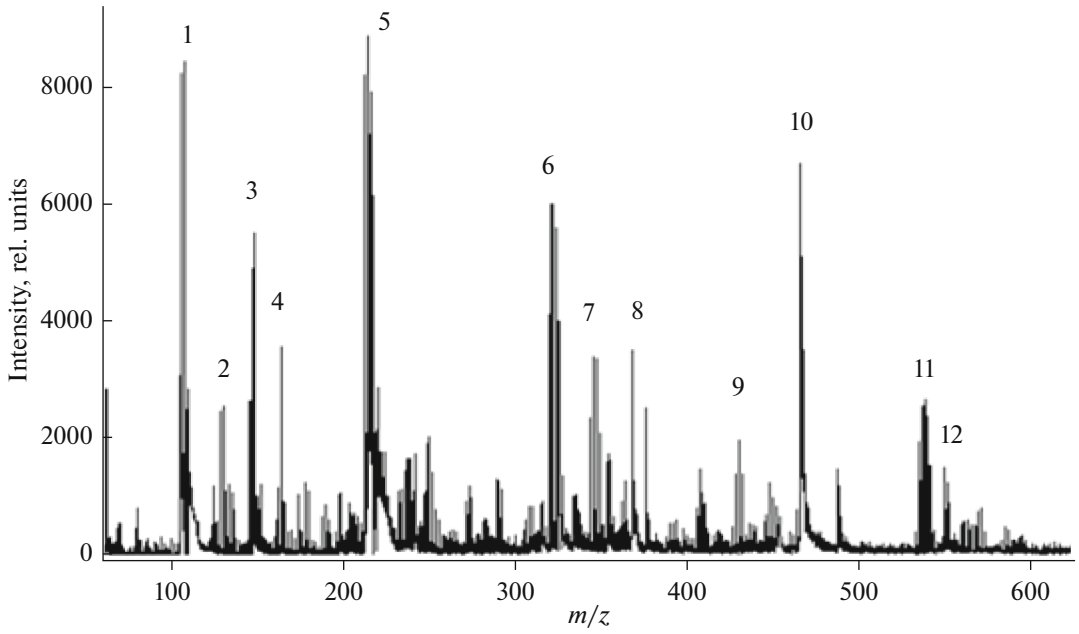

Fig. 1. Fragment of mass spectrum recorded for Ag NP RMS (ω = 8) within an m/z range of 60–600.

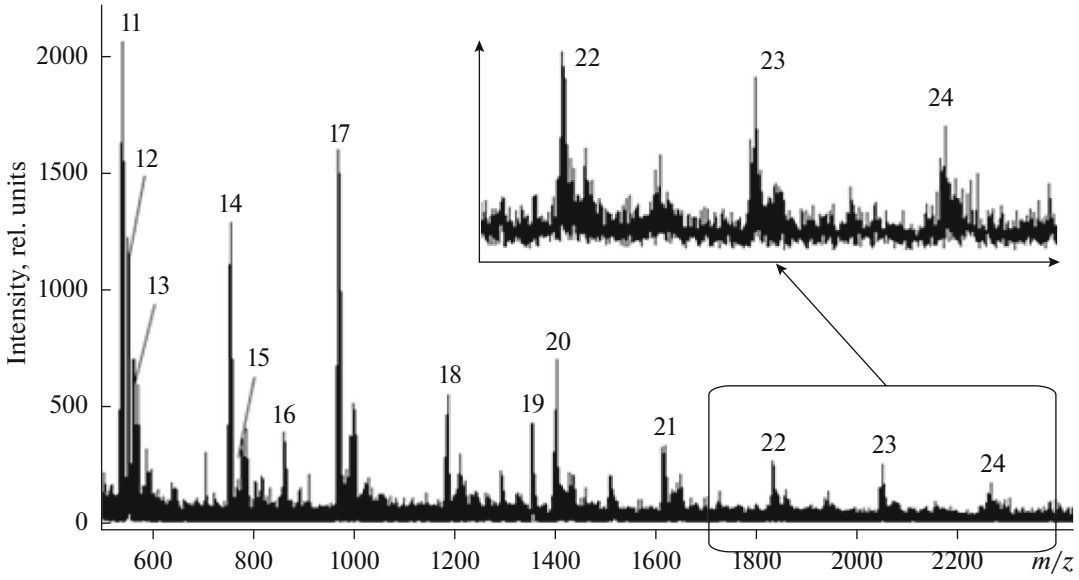

Fig. 2. Fragment of mass spectrum recorded for Ag NP RMS (ω = 8) within an m/z range of 500–3600.

(~420 nm) regions. At the same time, it is known that the surfactant (AOT) also absorbs light at a wavelength of 250 nm [13]. Therefore, silver nanoparticles were detected at a wavelength of 420 nm to avoid a complex chromatographic profile when performing the SEC studies.

Figure 4 shows chromatograms obtained for silver NPs in RMS with ω = 8 in different time periods after their synthesis. The corresponding values of the particle sizes in the studied solutions are presented in Table 2.

As is seen from the chromatogram measured for silver NPs in the RMS a week after the synthesis (Fig. 4a), the solution with ω = 8 contains only the fraction of fine particles. On the 92nd day after the synthesis (Fig. 4b), a fraction of coarse particles with retention time t_R = 8.34 min and particle size d_{max} = 19.5 nm arises. On the 364th day (Fig. 4c) the particle sizes of the coarse fraction are markedly decreased;

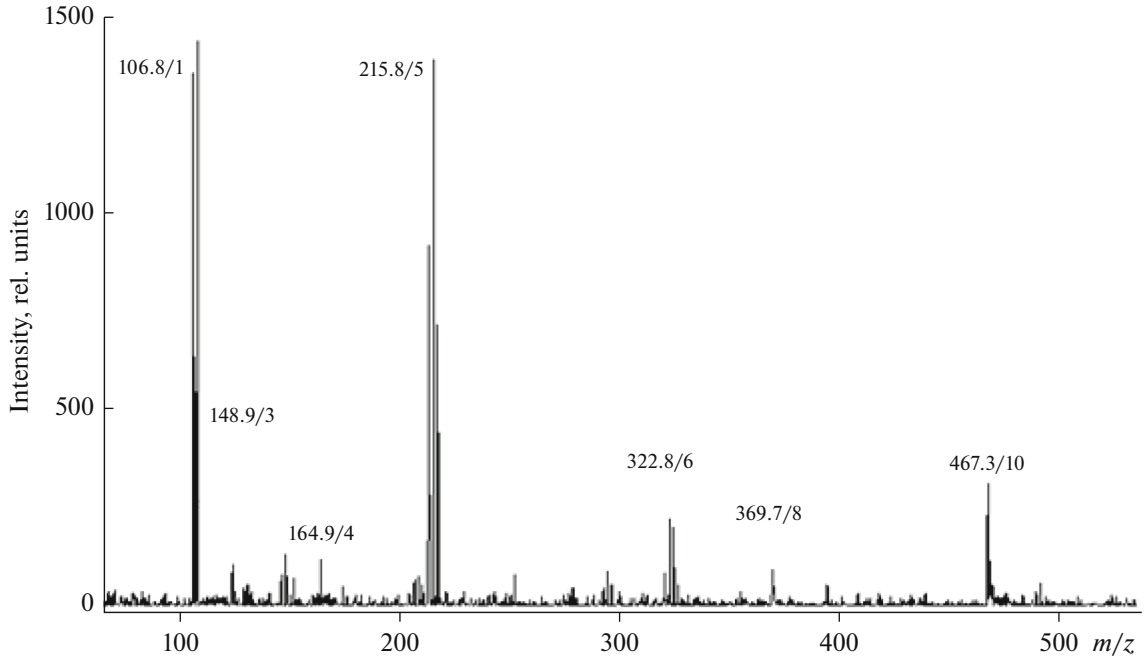

Fig. 3. Fragment of mass spectrum recorded for $Ag[NH_3]_2NO_3$ RMS (ω = 8) within an *m/z* range of 60–3600.

hence, the formation of this fraction in an RMS with ω = 8 is a reversible process.

The obtained SEC data were used to plot the size distribution curves of the detected particles for all samples (the graphical dependences of the percentage of particles on their sizes). The particle size distributions obtained for RMSs are exemplified in Fig. 5 (silver NPs in an RMS containing a single fraction) and Figs. 6 and 7 (silver NPs in RMSs containing two fractions of the particles). Table 3 presents some generalized data and the ranges of particle sizes in both fractions of all studied samples.

As follows from the data in Table 3, the particle sizes rather synchronously vary with time in all studied solutions except for the solution with ω = 20. The smallest sizes are observed for the first several months after the synthesis; then, they somewhat grow. In the case of the solution with the degree of hydration ω = 20, an increase in the particle sizes is observed only on the 245th day. At the same time, no increase in the particle sizes of the fine fraction is seen in all studied samples, thereby confirming that they are rather stable for a long time. The formation of the coarse particle fraction with time was not observed in all studied solutions. The largest particle sizes of this fraction were inherent in the solution with ω = 20. However, as for the particles of the fine fraction, no substantial increase in their sizes with time was recorded in this case. On the contrary, as is seen from Table 3, they are sometimes dissolved, and it may be concluded that the particles of the coarse fraction are aggregates of the particles of the fine fraction, and these particles retain the stabilizing shells formed by molecules of the surfactant (AOT). It should be noted that the reversible formation of the particles of the coarse fraction is, to a higher extent, characteristic of NPs in RMSs with higher values of ω = 8, 16, and 20. The range of the initial concentrations of silver ions (before the radiochemical reduction) in these RMSs was 6.5–16.2 mM. For NPs in RMSs with ω = 2 and 4, the initial silver salt concentration was 1.6–3.2 mM, and almost no coarse particles were formed in them. Accordingly, as the initial concentration of the silver salt, which is the precursor of the NPs, in an RMS increases, the final nanoparticle concentration in the RMS also increases, thus leading to a rise in the amount of stabilized NP aggregates in the solution.

Thus, RMSs with the degrees of hydration ω = $[H_2O]/[AOT]$ below 20 may contain one or two fractions of silver NPs. These particles are represented by reverse micelles containing Ag NPs in an aqueous pool. The particle sizes of the first fraction are in a range of 1–6 nm. They are stable systems that remain to be stable for a long time of storage. The particle sizes of the second fraction are in a range of 15–32 nm and reversibly vary within a range of 5–10 nm. These particles are aggregates of the fine-fraction particles.

For comparison with the data obtained in the LDI mode on the size distribution of clusters of silver nanoparticles, the number of silver atoms in one micelle was calculated from the micelle size determined by SEC. The calculation has shown that one Ag NP must contain up to 100 Ag atoms; i.e., the ionization either is accompanied by a substantial fragmenta-

Table 1. Ions and adducts presumably present in the mass spectra measured for $Ag[NH_3]_2NO_3$ and Ag NPs in RMSs in the mode of positive ion registration

Peak no.	*m/z*, Da	Empirical formula	Assumed ion (adduct)
1	106.6	Ag_1	Ag^+
2	129.7	Ag_1Na_1	$Ag{\cdot}Na^+$
3	148.7	$O_3Na_3S_1$	$Na_2SO_3{\cdot}Na^+$
4	164.8	$O_3Na_2S_1K_1$	$Na_2SO_3{\cdot}K^+$
5	215.7	Ag_2	$Ag{\cdot}Ag^+$
6	322.7	Ag_3	$Ag_2{\cdot}Ag^+$
7	346.7	$H_1Na_1Ag_3$	$Ag_3{\cdot}Na_1{\cdot}H^+$
8	369.6	–	Unidentified
9	431.7	Ag_4	$Ag_3{\cdot}Ag^+$
10	467.3	$C_{20}H_{37}O_7Na_2S_1$	Sodium bis(2-thylhexyl) sulfosuccinate$\cdot Na^+$
11	538.7	Ag_5	$Ag_4{\cdot}Ag^+$
12	553.3	$C_{20}H_{37}O_7Na_1S_1Ag_1$	Sodium bis(2-ethylhexyl) sulfosuccinate$\cdot Ag^+$
13	562.7	$H_1Na_1Ag_5$	$Ag_5{\cdot}Na_1{\cdot}H^+$
14	754.6	Ag_7	$Ag_6{\cdot}Ag^+$
15	778.6	$H_1Na_1Ag_7$	$Ag_7{\cdot}Na_1{\cdot}H^+$
16	863.5	Ag_8	$Ag_7{\cdot}Ag^+$
17	970.4	Ag_9	$Ag_8{\cdot}Ag^+$
18	1186.3	Ag_{11}	$Ag_{10}{\cdot}Ag^+$
19	1356.0	$C_{60}H_{111}O_{21}Na_4S_3$	(Sodium bis(2-ethylhexyl) sulfosuccinate)$_3{\cdot}Na^+$
20	1402.2	Ag_{13}	$Ag_{12}{\cdot}Ag^+$
21	1618.1	Ag_{15}	$Ag_{14}{\cdot}Ag^+$
22	1833.9	Ag_{17}	$Ag_{16}{\cdot}Ag^+$
23	2051.7	Ag_{19}	$Ag_{18}{\cdot}Ag^+$
24	2265.7	Ag_{21}	$Ag_{20}{\cdot}Ag^+$

tion of NPs or it may be assumed that the synthesis of nanoparticles is uncompleted, and the aqueous pool contains finer particles. Another variant for the appearance of the low-molecular-mass silver clusters with the number of atoms below 21 revealed by the mass spectrometry method may be their formation as intermediate products from which Ag NPs are obtained in the course of the synthesis. For example, the formation of such nanoclusters with numbers of atoms smaller than 25 as an intermediate stage of the synthesis was established by the LDI mass spectrometry during the synthesis of gold NPs [28].

CONCLUSIONS

Size-exclusion chromatography has been employed to determine the sizes of silver nanoparticles in reverse micelles for a year after their synthesis. It has been found that these particles compose actually two fractions. The sizes of the first fraction are in a range of 1–6 nm and remain almost unchanged with time, thereby indicating their high stability. The coarse fraction has particle sizes of 15–32 nm, which reversibly vary in the course of long-term storage within a range of ±10 nm. The formation of the coarse-fraction particles is more characteristic for NPs in RMSs with high

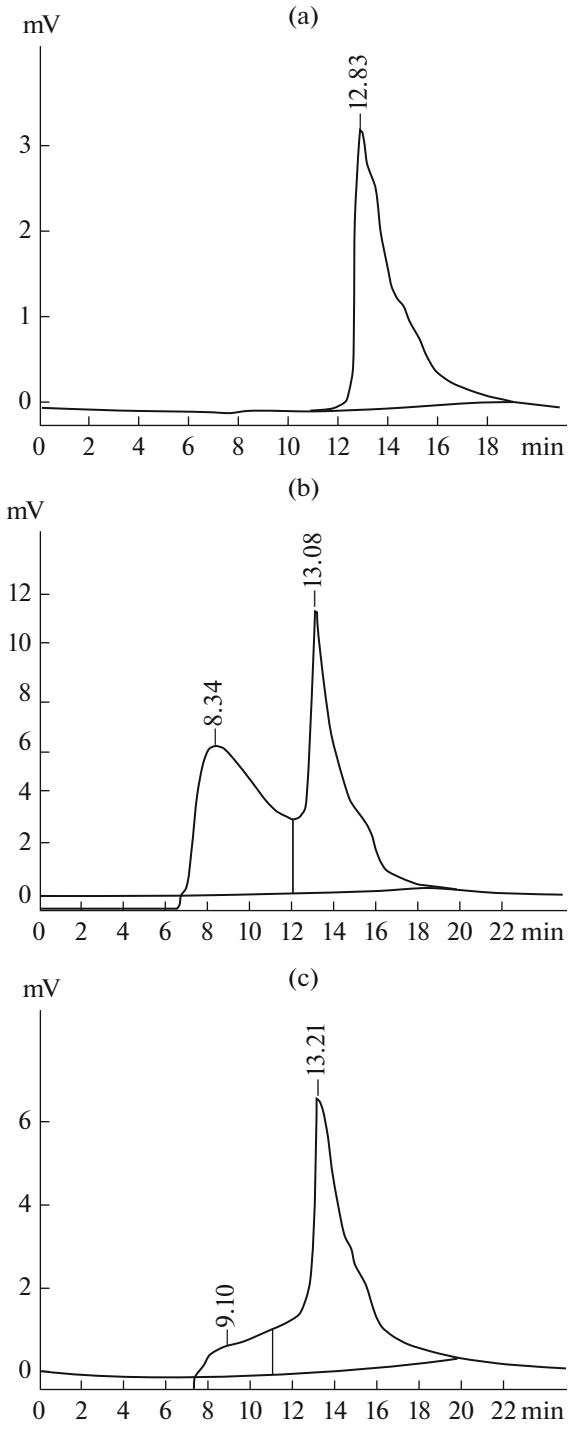

Fig. 4. Examples of size-exclusion chromatograms measured for silver NP RMS (ω = 8) on (a) 8th, (b) 92nd, and (c) 364th day after the synthesis.

values of ω = 8, 16, and 20. In RMSs with ω = 2 and 4, almost no coarse particles are formed. On the basis of the obtained sizes and their variations with time, it has been assumed that Ag NPs in RMSs with ω values lower than 20 are stable systems, other synthesis conditions being equal. The particles of the coarse fraction are represented by aggregates of fine-fraction particles, which retain their stabilizing shells formed by molecules of the surfactant (AOT).

The comparison between the number of silver atoms introduced into a reverse micellar system before the synthesis and the number of silver atoms observed

Table 2. Size ranges of studied Ag NPs in RMSs according to the SEC data

Duration of silver NP RMS storage, days		ω = 8	
		d of fine particles, nm	*d* of coarse particles, nm
8	Total size range	1.9–3.7	–
	Maximum	3.5	–
92	Total size range	1.9–28.6	
	Size range of particles with content of ≥2%	2.0–3.3	9.8–24.5
	Maximum	3.1	19.5
364	Total size range	1.9–24.9	
	Size range of particles with content of ≥1%	1.9–9.7	
	Maximum	2.9	

Table 3. Sizes of silver particles detected in RMSs according to SEC data

Duration of RMS storage, days		ω = 2	ω = 4	ω = 8	ω = 16	ω = 20
6	*d* of fine particles, nm	1.6–3.6	1.6–3.6	1.6–3.6	1.4–3.3	1.4–3.3
8	d of fine particles, nm	1.6–3.6	1.6–3.6	1.9–3.7	1.6–3.6	1.5–3.6
14	*d* of fine particles, nm	1.6–3.6	1.6–3.5	1.8–3.6	1.8–3.6	1.6–3.5
	d of coarse particles, nm	14.3–15.4	–	–	13.3–15.4	–
64	*d* of fine particles, nm	1.7–3.5	1.8–3.8	2.2–29.7	1.6–3.5	1.8–3.6
	d of coarse particles, nm	–	–		19.5–30.8	22.7–26.5
92	*d* of fine particles, nm	1.8–3.6	1.8–3.6	2.2–28.6	1.6–3.5	1.9–3.9
	d of coarse particles, nm	–	–		18.1–26.5	22.7–26.5
161	*d* of fine particles, nm	2.0–7.8	1.9–4.8	2.3–29.7	1.6–3.5	2.0–4.4
	d of coarse particles, nm	–	–		16.1–29.7	23.6–32.0
364	*d* of fine particles, nm	1.7–3.6	1.8–3.8	1.9–9.7	2.0–4.1	2.0–3.8
	d of coarse particles, nm	–	–	–	20.2–21.8	–
Average range	*d* of fine particles, nm	1.7–3.8	1.7–3.7	2.0–4.7	1.7–3.6	1.8–3.7
	d of coarse particles, nm	14.3–15.4	21.0–26.4	4.8–28.1	18.2–25.3	22.5–28.9

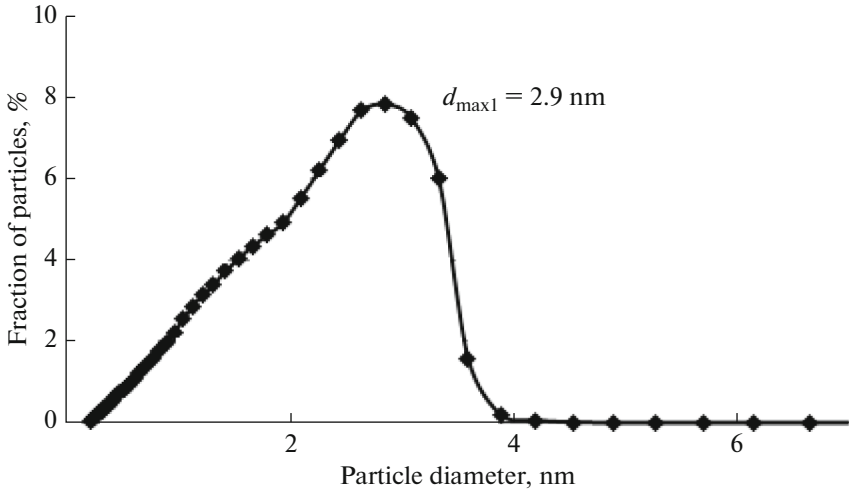

Fig. 5. Size distribution of Ag NPs detected in RMS (ω = 2) on the 37th day after the synthesis (λ = 420 nm).

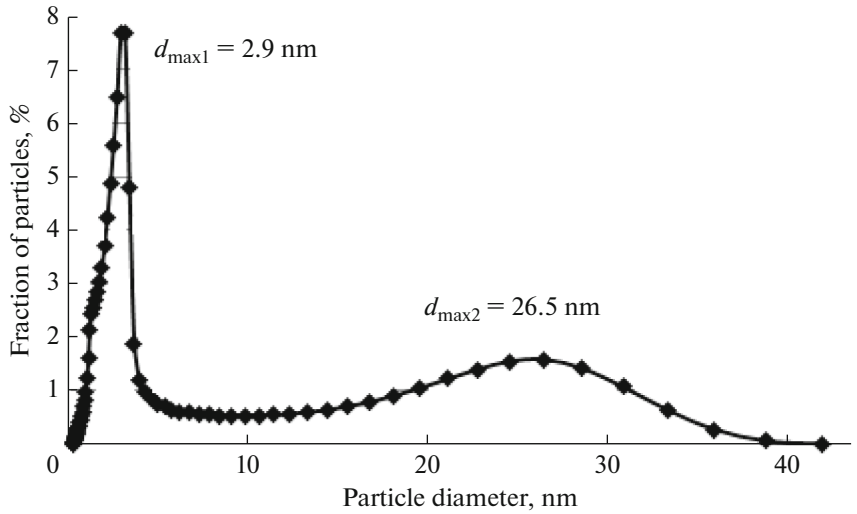

Fig. 6. Size distribution of Ag NPs detected in RMS (ω = 16) on the 64th day after the synthesis (λ = 420 nm).

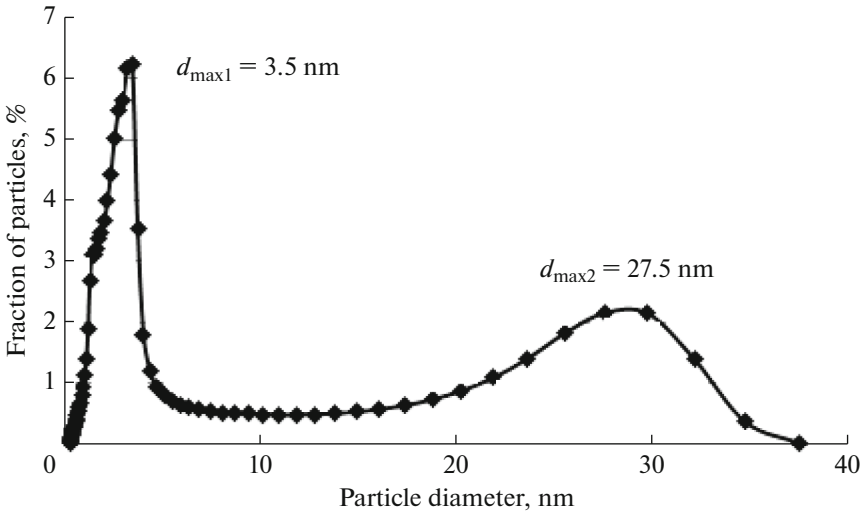

Fig. 7. Size distribution of Ag NPs detected in RMS (ω = 20) on the 245th day after the synthesis (λ = 420 nm).

by mass spectroscopy gives grounds to assume that either the synthesis is not completed or the ionization of coarse nanoparticles may be accompanied by their disruption into smaller fragments.

FUNDING

This work was supported by the Ministry of Science and Higher Education of the Russian Federation.

CONFLICT OF INTEREST

The authors declare that they have no conflicts of interest.

REFERENCES

1. Ershov, B.G., *Ross. Khim. Zh.,* 2001, vol. 45, no. 3, p. 20.
2. Gubin, S.P., Koksharov, Y.A., Khomutov, G.B., and Yurkov, G.Y., *Russ. Chem. Rev.,* 2005, vol. 74, no. 6, p. 489. https://doi.org/10.1070/rc2005v074n06abeh000897
3. Kwiczak-Yiğitbaşl, J., Demir, M., Ahan, R.E., Canll, S., Şafak Şeker, U.Ö., and Baytekin, B., *ACS Sustainable Chem. Eng.,* 2020, vol. 8, no. 51, p. 18879. https://doi.org/10.1021/acssuschemeng.0c05493
4. Xiao, S., Xu, W., Ma, H., and Fang, X., *RSC Adv.,* 2012, vol. 2, no. 1, p. 319. https://doi.org/10.1039/c1ra00127b

5. Baghayeri, M., Namadchian, M., Karimi-Maleh, H., and Beitollahi, H., *J. Electroanal. Chem.,* 2013, vol. 697, p. 53. https://doi.org/10.1016/J.JELECHEM.2013.03.011
6. Abbasi, A.R., Kalantary, H., Yousefi, M., et al., *Ultrason. Sonochem.,* 2012, vol. 19, no. 4, p. 853. https://doi.org/10.1016/j.ultsonch.2011.11.011
7. Nakamura, S., Sato, M., Sato, Y., et al., *Int. J. Mol. Sci.,* 2019, vol. 20, no. 15, p. 3620. https://doi.org/10.3390/ijms20153620
8. Liu, L.T., Li, Y.Z., Yu, K.P., et al., *Mater. Res. Lett.,* vol. 9, no. 6, p. 270. https://doi.org/10.1080/21663831.2021.1894613
9. Krutyakov, Y.A., Kudrinskiy, A.A., Olenin, A.Y., and Lisichkin, G.V., *Russ. Chem. Rev.,* 2008, vol. 77, no. 3, p. 233. https://doi.org/10.1070/rc2008v077n03abeh003751
10. El-Batal, A.I., Elkodous, M., El-Sayyad, G.S., et al., *Int. J. Biol. Macromol.,* 2020, vol. 165, p. 169. https://doi.org/10.1016/j.ijbiomac.2020.09.160
11. Eastoe, J., Hollamby, M.J., and Hudson, L., *Adv. Colloid Interface Sci.,* 2006, vol. 128, p. 5. https://doi.org/10.1016/j.cis.2006.11.009
12. Bulavchenko, A.I., Podlipskaya, T.Y., Demidova, M.G., et al., *Solvent Extr. Ion Exch.,* 2020, vol. 38, no. 4, p. 455. https://doi.org/10.1080/07366299.2020.1733747
13. Shafigulina, A.D., Revina, A.A., Platonova, N.P., Borovikova, S.A., and Buryak, A.K., *Colloid J.,* 2019, vol. 81, no. 3, p. 292. https://doi.org/10.1134/S1061933X19030128
14. Chiang, C.L., *J. Colloid Interface Sci.,* 2001, vol. 239, no. 2, p. 334. https://doi.org/10.1006/jcis.2001.7590
15. Larionov, O.G., Revina, A.A., Belyakova, L.D., Volkov, A.A., and Ponomarev, K.V., *Prot. Met. Phys. Chem. Surf.,* 2011, vol. 47, no. 6, p. 748. https://doi.org/10.1134/S207020511106013X
16. Harkness, K.M., Cliffel, D.E., and McLean, J.A., *Analyst,* 2010, vol. 135, no. 5, p. 868. https://doi.org/10.1039/b922291j
17. Guo, J., Kumar, S., Bolan, M., et al., *Anal. Chem.,* 2012, vol. 84, no. 12, p. 5304. https://doi.org/10.1021/ac300536j
18. Kim, B.H., Chang, H., Hackett, M.J., et al., *Bull. Korean Chem. Soc.,* 2014, vol. 35, no. 3, p. 961. https://doi.org/10.5012/bkcs.2014.35.3.961
19. Bustos, A.R.M., Encinar, J.R., and Sanz-Medel, A., *Anal. Bioanal. Chem.*, 2013, vol. 405, no. 17, p. 5637. https://doi.org/10.1007/s00216-013-7014-y
20. Liu, F.K. and Chang, Y.C., *Chromatografia,* 2011, vol. 74, no. 11, p. 767. https://doi.org/10.1007/s10337-011-2139-7
21. Kuz'min, V.I., Gadzaov, A.F., Tytik, D.L., Busev, S.A., and Revina, A.A., *Colloid J.,* 2015, vol. 77, no. 4, p. 458. https://doi.org/10.1134/S1061933X15040110
22. Kuz'min, V.I., Gadzaov, A.F., Tytik, D.L., Busev, S.A., and Revina, A.A., *Colloid J.,* 2015, vol. 77, no. 4, p. 473. https://doi.org/10.1134/S1061933X15040122
23. Egorova, E.M. and Revina, A.A., *Colloids Surf., A,* 2000, vol. 168, no. 1, p. 87. https://doi.org/10.1016/S0927-7757(99)00513-0
24. Shafigulina, A.D., Larionov, O.G., Revina, A.A., Busev, S.A., Ponomarev, K.V., and Larionova, A.O., *Prot. Met. Phys. Chem. Surf.,* 2014, vol. 50, no. 6, p. 755. https://doi.org/10.1134/S2070205114060197
25. Yau, W.W., Kirkland, J.J., and Bly, D.D., *Modern Size-Exclusion Liquid Chromatography. Practice of Gel Permeation and Gel Filtration Chromatography,* New York: Wiley, 2009, 2nd ed.
26. Boryak, O.A., Kosevich, M.V., Chagovets, V.V., and Shelkovsky, V.S., *J. Anal. Chem.*, 2017, vol. 72, no. 13, p. 1289. https://doi.org/10.1134/S1061934817130032
27. Kuzmin, V.I., Tytik, D.L., Belashchenko, D.K., and Sirenko, A.N., *Colloid J.,* 2008, vol. 70, no. 3, p. 284. https://doi.org/10.1134/S1061933X08030058
28. Wu, Z., Gayathri, C., Gil, R.R., and Jin, R., *J. Am. Chem. Soc.*, 2009, vol. 131, no. 18, p. 6535. https://doi.org/10.1021/ja900386s

Translated by A. Kirilin